*Int. J. Electrochem. Sci.*, 14 **(2019)** 5629 – 5636, doi: 10.20964/2019.06.50

International Journal of
ELECTROCHEMICAL
SCIENCE
www.electrochemsci.org

*Short Communication*

# Rose-like $Bi_2MoO_6$ Microsphere as Electrode Material for High Performance Supercapacitor

*Xuemin Yu*[*], *Ying Sun, Xueqin Zhang and Baoping Lin*

School of Chemistry and Chemical Engineering, Southeast University, Nanjing 211189, China
[*]E-mail: lilycc1031@163.com

*Received:* 6 February 2019 / *Accepted:* 28 March 2019 / *Published:* 10 May 2019

Rose-like $Bi_2MoO_6$ microsphere has been successfully prepared by a typical hydrothermal method, and it is the first time that the material of this morphology has been studied for its electrochemistry properties. The rose-like microsphere with a mean a hierarchical structure is composed of plenty of nanoplates [1], and possesses an excellent specific surface area ($S_{BET}$) of 63 $m^2/g$ and total pore volume ($T_{tot}$) of 0.2336 $cm^3/g$. As an electrode material for supercapacitor, it delivers a large specific capacitance of 828 F/g at 1 A/g, and displays a good rate performance which the 84% capacitance can be hold as the current density increases tenfold [2], exhibits good cycle stability with the capacitance retention of about 57.04% over 1000 repeated charging/discharging process at 10 A/g. The desirable electrochemical performance may be related to the synergistic effect of rose-like microsphere structure and porous structure. These results demonstrate that rose-like $Bi_2MoO_6$ microsphere is a promising electrode material for high performance supercapacitor [2].

**Keywords:** $Bi_2MoO_6$; Hydrothermal method; Supercapacitor; Specific capacitance; Rate performance.

## 1. INTRODUCTION

Nowadays, with the increasing challenge of energy crisis and environmental pollution, sustainable and green energy storage and conversion systems are emergently demanded [1, 2]. Among the novel energy storage devices, supercapacitor has attracted more and more attentions due to its various merits, such as higher power densities, superior rate performance, longer cycle life and no memory effect [2-5]. Pseudocapacitor, one kind of the supercapacitor, stores energy by the Faradic reaction occurred at the surface or near the surface regions of the electrode materials [6]. Thus, the electrochemical performance of pseudocapacitor mainly counts on the electrode materials adopted [7]. And considerable efforts have been made to design/fabricate advanced faradaic electrode materials with high electrochemical performance, such as transition metal oxides/hydroxides and conducting polymers [8-11]. However, for most of the bulk pseudocapacitance electrode materials, only the surface regions can

be made full use to produce capacitance, resulting in poor electrochemical performance [12]. Luckily, it was reported that nanostructured materials with hierarchically porous structures can introduce new reactions, increase the active materials/electrolyte contact areas, shorten the path lengths for electrolyte ions and electrons, and suppress the pulverization during electrochemical reaction process [13-15]. Therefore, to gain excellent electrochemical performances, the nanostructured materials with hierarchical porous structure are more essential [12, 16].

$Bi_2MoO_6$, one of the Bismuth-based materials, is generally regarded as one of the promising electrode material, due to its stable crystal structure, easy fabrication, nontoxicity and moderate band gap [16]. Recently the application of $Bi_2MoO_6$ nanomaterials has expanded into the field of energy storage, especially supercapacitors. However, they still suffer from low specific capacitance under high current density and poor cycle stability, which is a hindrance to its practical application [17]. Therefore, more effort is needed to improve related performance, and it is meaningful to synthesize $Bi_2MoO_6$ materials with excellent specific surface area ($S_{BET}$) to further enhance the electrical performances. To the best of our knowledge, the rose-like $Bi_2MoO_6$ microsphere with a hierarchical structure has been rarely reported, and the electrochemical properties has been also rarely studied [16-18].

In this context, rose-like nanostructured $Bi_2MoO_6$ with microsphere with hierarchical structure has been successfully prepared and first used as electrode material for supercapacitor. Finally, the samples exhibited superior electrochemical performance for supercapacitor.

## 2. EXPERIMENTAL

### *2.1. Preparation of rose-like $Bi_2MoO_6$ microsphere*

$Bi_2MoO_6$ microsphere was prepared by a typical procedure according to the literature [13]. Specifically, $Bi(NO_3)_3$•$5H_2O$ (2 mmol) and $Na_2MoO_4$•$2H_2O$ (1 mmol) were added into 10 mL of ethylene glycol in sequence with sonication and vigorous magnetic stirring for 15 min. Afterwards, 25 mL ethanol was slowly poured into the above solution with constant stirring for 15 min [19]. Finally, the hybridized solution was hydrothermal treated at 160℃ for 12h [16]. The solid product was filtered and rinsed with deionized water and ethanol for several times, and then the product was obtained by drying at 60℃ under vacuum overnight.

### *2.2. Characterization of $Bi_2MoO_6$ microsphere*

X-ray diffraction (XRD) pattern was performed on a Rigaku Smart-Lab X-ray diffractometer at a scan rate of 10 ℃/min. X-ray photoelectron spectroscopy (XPS) was recorded by Thermo escalab 250Xi. The morphology of $Bi_2MoO_6$ was obtained by scanning electron microscope (SEM, JSM-6390LV, JEOL) and transmission electron microscopy (TEM, Philips Tecnai-12). Nitrogen adsorption-desorption isotherm was measured to characterize the pore structure parameters using a Quantachrome Autosorb-iQ-MP analyzer at 77 K.

### *2.3. Electrochemical measurements*

The working electrode was fabricated by mixing $Bi_2MoO_6$, acetylene black and polytetrafluoroethylene at a mass ratio of 8:1:1 with N-methylpyrrolidinone as solvent homogenously [20]. The slurry mixture was then coated onto the nickel foam substrate and dried at 80 ℃ overnight under vacuum. Three-electrode cell assembled with a working electrode, a platinum foil counter electrode, Hg/HgO reference electrode and 6 M KOH solution as electrolyte was used for evaluating the electrochemical performance of the $Bi_2MoO_6$ array, and the active material mass loading of the single electrode is about 4.32 mg [21]. All the electrochemical measurements, such as galvanostatic charge/discharge (GCD), cyclic voltammetry (CV) were recorded with the electrochemical working station (CHI 660e). The single specific capacitance of the electrode was calculated from the following equation [22] (1):

$$C_M = (I \times \Delta t) / (m \times \Delta V) \quad (1)$$

Where $C_m$ is the gravimetric capacitance (F/g), $I$ is the constant current (A), m is the mass (g) of the active material, $\Delta t$ is the discharge time and $\Delta V$ is the voltage window.

## 3. RESULTS AND DISCUSSION

### *3.1. Microstructure and morphology characterization*

XRD measurement has been carried out to characterize the crystal structure of $Bi_2MoO_6$ sphere. As exhibited in Fig. 1a, several clear and sharp diffraction peaks are observed, which agrees well with the literature [13]. XPS has been used to confirm the element composition of $Bi_2MoO_6$. Fig. 1b shows that the elements of Bi, O, Mo and C can be clearly observed. As observed in Fig. 1c, two peaks centered at the binding energy of 158.8 eV and 164.2 eV can be assigned to the Bi $4f_{7/2}$ and Bi $4f_{5/2}$ of $Bi^{3+}$ [23-25]. The Mo 3d spectrum in Fig. 1d demonstrates that the two peaks located at the binding energy of 231.9 and 235.3 eV corresponds to Mo $3d_{3/2}$ and Mo $3d_{5/2}$ of $Mo^{6+}$, respectively. The two peaks in Fig. 1e may be related to the Bi-O bond and oxygen bonded to the adventitious carbon species [26]. The results above both demonstrate that $Bi_2MoO_6$ has been successfully prepared.

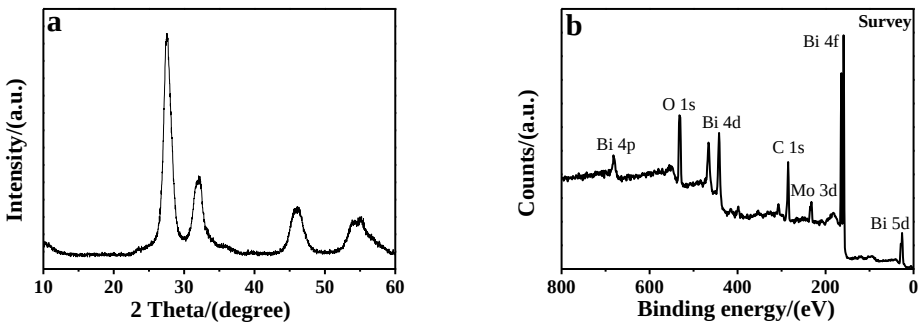

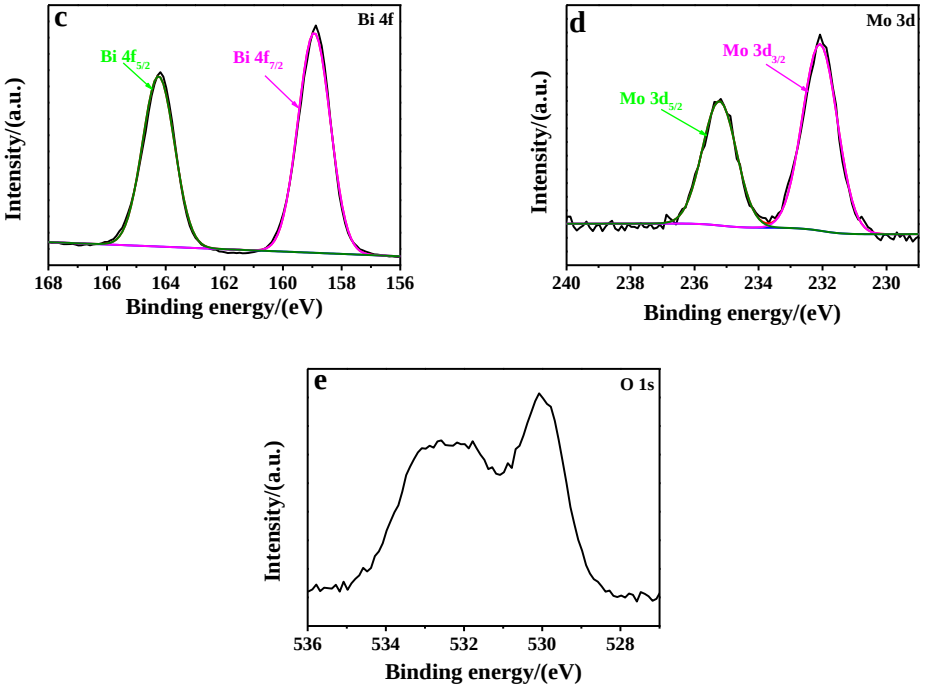


**Figure 1**. XRD pattern (a) and XPS spectra of $Bi_2MoO_6$: (b) survey, (c) Bi 4f, (d) Mo 3d and (e) O 1s.

SEM and TEM have been used to observe the micromorphology of the $Bi_2MoO_6$. As clearly observed from Fig. 2a, the as prepared $Bi_2MoO_6$ exhibits rose-like microsphere structure with the mean diameter of about 1μm. From Fig. 2b, it can be observed that the sphere is constructed of plenty of nanoplates. Fig. 2c-e further shows the sphere structure of $Bi_2MoO_6$, which is composed of nanoplates. Moreover, the selected-area electron diffraction (inset in Fig. 2e) further indicates the polycrystalline nature of $Bi_2MoO_6$ [20]. The nitrogen adsorption-desorption isotherm and pore size distribution curve are demonstrated in Fig. 3. The obvious hysteresis loop reflects the mesoporous structure of $Bi_2MoO_6$, which may be ascribed to the space between nanoplates. Meanwhile, the pore size distributes from 2 nm to 25 nm. The $S_{BET}$ and $T_{tot}$ of $Bi_2MoO_6$ microsphere are 63 $m^2/g$ and 0.2336 $cm^3/g$, respectively. The nanostructured microsphere with porous structure may be beneficial to the enhancement of electrochemical performance of $Bi_2MoO_6$.

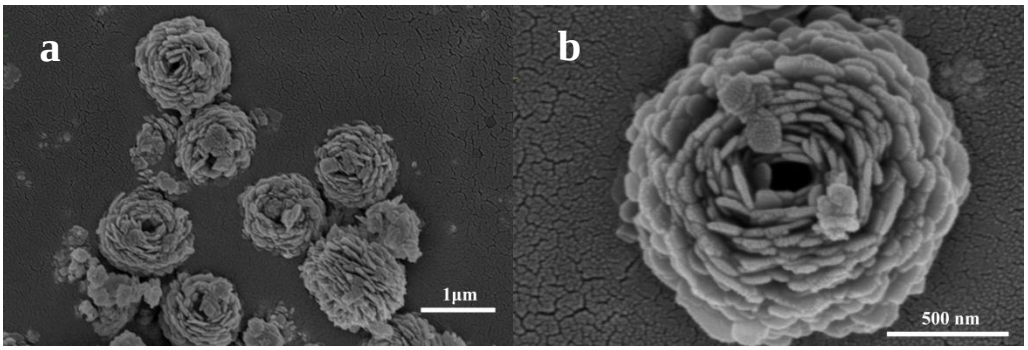

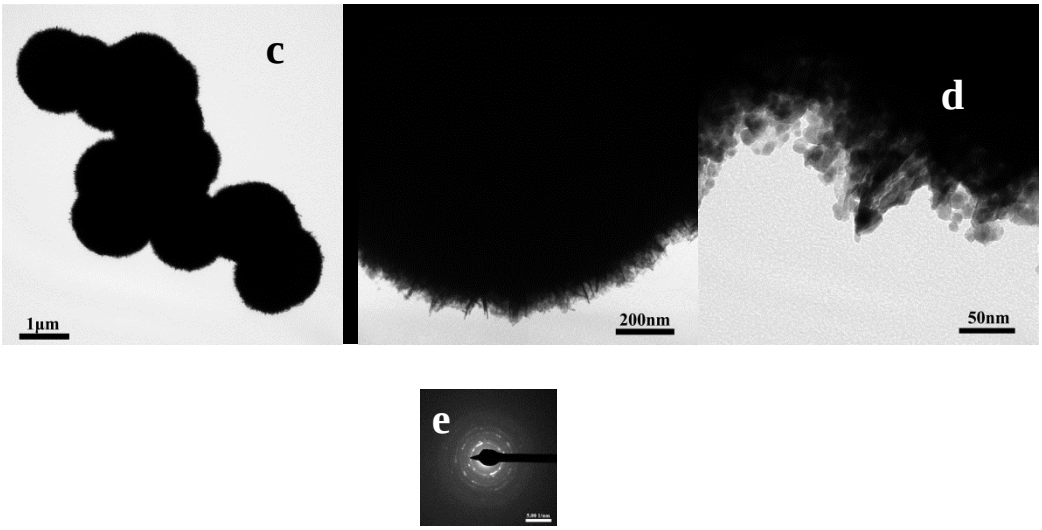


**Figure 2.** SEM images (a-b) and TEM images (c-e) of the $Bi_2MoO_6$.

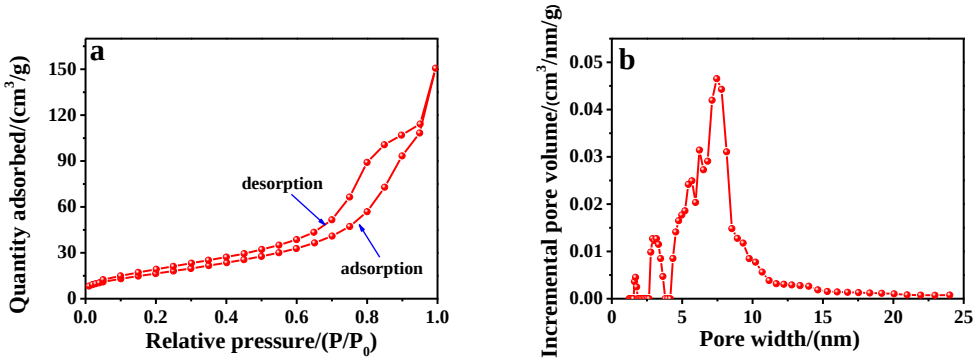


**Figure 3**-a. $N_2$ adsorption-desorption isotherms of carbon materials; b. Pore size distribution of carbon materials.

### *3.2. Electrochemical characterization*

To characterize the electrochemical performances, the as-prepared $Bi_2MoO_6$ microsphere has been investigated as an electrode material in a three-electrode system using 6 M KOH solution as electrolyte [24]. Fig. 4a depicts the CV curves of $Bi_2MoO_6$ measured at a series of scan rates of 10~80 mV $s^{-1}$ in the potential window of -1.0~0 V. The obvious redox peaks can be observed at various scan rates and the similar shape can be almost retained even at the high scan rate of 80 mV/s, which indicates the excellent rate property of $Bi_2MoO_6$ as electrode material [27].

Fig. 4b manifests the GCD curves of $Bi_2MoO_6$ as electrode material during the current density of 1~10 A/g. The obvious horizontal charge-discharge potential plateaus suggest the existence of Faradic reaction. The $C_m$ of $Bi_2MoO_6$ is as high as 828 F/g at 1 A/g, which is higher than that of hierarchical nanosheet-based $Bi_2MoO_6$ nanotubes (171.3 F/g, 0.585 A/g) [26], $Bi_2O_3$/activated carbon composite (466 F/g, 1 A/g) [27] and ultrathin $Bi_2O_3$ nanowires (691.3 F/g, 2 A/g) [28]. As shown in Fig. 4c and Table.1, the $C_m$ values present a decreasing trend as the current density increases. But the specific

capacitance can still maintain 696 F/g at 10 A/g with the rate performance of 84%, which is 34% over γ-$Bi_2MoO_6$ nanoplates (519 F/g at a scan rate of 2 mV/s) [29] and about 200% greater than $Bi_2MoO_6$ hollow microspheres (146F/g at 5A/g) [30], demonstrating the outstanding rate capability.

The cycling performance is shown in Fig. 4d. The long-term cycles of $Bi_2MoO_6$ as electrode material has been evaluated by continuous GCD test up to 1000 cycles at 10 A/g. The capacitance retention is 57.04% over 1000 repeated charging/discharging process. The excellent electrochemical performance may be ascribed to the nanostructured microsphere assembled with plenty of nanoplates and porous structure of $Bi_2O_2CO_3$.

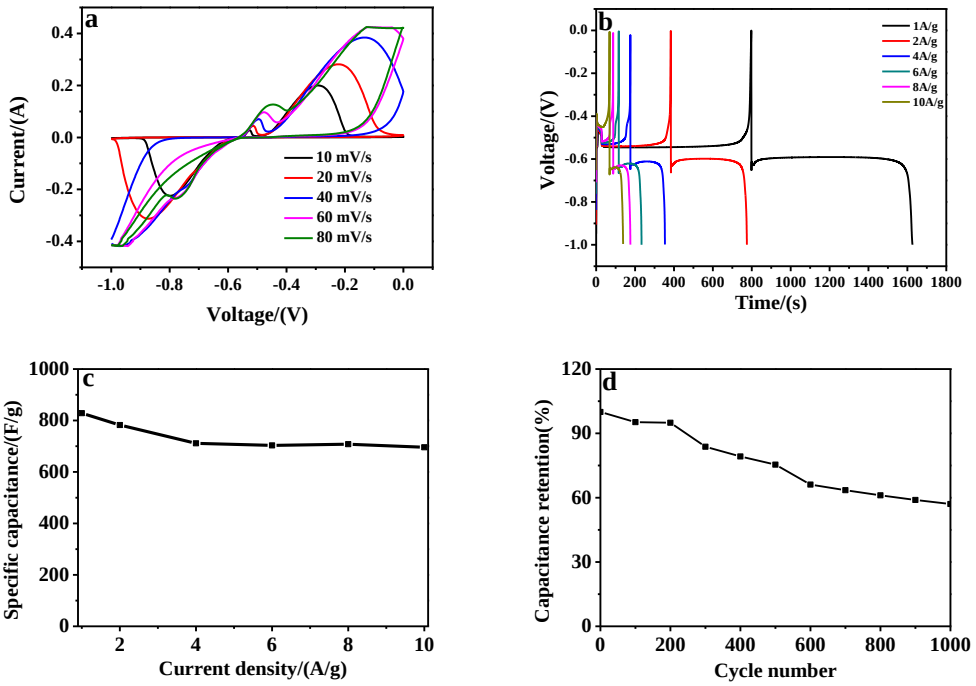


**Figure 4.** CV curves of $Bi_2MoO_6$ as electrode material at different scan rates (a); Charge-discharge curves of $Bi_2MoO_6$ as electrode material at different current densities (b); Current density versus specific capacitance (c); Cycle performance of $Bi_2MoO_6$ as electrode material at 10 A/g (d).

**Table 1.** Specific capacitances of $Bi_2MoO_6$ as electrode material at different current densities

| Samples | Specific capacitance/(F/g) | | | | | |
|---|---|---|---|---|---|---|
| | 1 /(A/g) | 2 /(A/g) | 4 /(A/g) | 6 /(A/g) | 8 /(A/g) | 10 /(A/g) |
| $Bi_2MoO_6$ | 828 | 782 | 711 | 703 | 708 | 696 |

## 4. CONCLUSIONS

In summary, rose-like $Bi_2MoO_6$ microsphere has been synthesized by a typical hydrothermal method, which with an average diameter of about 1μm, is assembled of nanoplates. It possesses porous

structure with the $S_{BET}$ of 63 $m^2/g$ and $T_{tot}$ of 0.2336 $cm^3/g$. When used for supercapacitor, it obtains a high $C_m$ of 828 F/g at 1 A/g, displays a good rate performance (84%,1~10 A/g), exhibits good cyclability with the capacitance retention of about 57.04% during 1000 repeated charging/discharging process at 10 A/g. The rose-like $Bi_2MoO_6$ microsphere is a promising electrode material for supercapacitors.

ACKNOWLEDGEMENTS
This work was financially supported by the National Natural Science Foundation of China (Grant Nos. 21374016, 21304018), the Jiangsu Provincial Natural Science Foundation of China (BK20130619, BK20130617) and the Fundamental Research Funds for the Central Universities.

**References**

1. G. Zhao, C. Chen, D. Yu, L. Sun, C. Yang, H. Zhang, Y. Sun, F. Besen and M. Yu, *Nano Energy*., 47 (2018) 547.
2. A.M. Elshahawy, C. Guan, W. Zang, S. Ding, Z. Kou, S.J. Pennycook, N. Yan and J. Wang, *ACS Appl. Energy Mater.*, 2(1) (2018) 616.
3. X. Wu, L. Meng, Q. Wang, W. Zhang and Y. Wang, *Solar Energy Mater. Sol. Cells*., 174 (2018) 325.
4. L. Li, X. Liu, C. Liu, H. Wan, J. Zhang, P. Liang, H. Wang and H. Wang, *Electrochim. Acta.*, 259 (2018) 303.
5. W. Kang, B. Lin, G. Huang, C. Zhang, W. Hou, Y. Yao, B. Xu and B. Xing, *J. Mater. Sci.: Mater Electron*., 29(4) (2018) 3340.
6. W. Kang, B. Lin, G. Huang, C. Zhang, Y. Yao, W. Hou, B. Xu and B. Xing, *J. Mater. Sci.: Mater. Electron*., 29(8) (2018) 6361.
7. Y. Tingting, L. Ruiyi, L. Zaijun, G. Zhiguo, W. Guangli and L. Junkang, *Electrochim. Acta.*, 211 (2016) 59.
8. Y. Tingting, L. Ruiyi, L. Xiaohuan, L. Zaijun, G. Zhiguo, W. Guangli and L. Junkang, *Electrochim. Acta*., 187 (2016) 143.
9. X. He, Q. Liu, J. Liu, R. Li, H. Zhang, R. Chen and J. Wang, *J. Alloys Compd*., 724 (2017) 130.
10. D. Guo, M. Zhang, Z. Chen and X. Liu, *Mater. Res. Bull*., 96 (2017) 463.
11. X. Wu, Z. Han, X. Zheng, S. Yao, X. Yang and T. Zhai, *Nano Energy.*, 31 (2017) 410.
12. J. Lin, Y. Liu, Y. Wang, H. Jia, S. Chen, J. Qi, C. Qu, J. Cao, W. Fei and J. Feng, *Ceram. Int.*, 43(17) (2017) 15410.
13. S. Zhu, L. Li, J. Liu, H. Wang, T. Wang, Y. Zhang, L. Zhang, R.S. Ruoff and F. Dong, *ACS Nano.*, 12(2) (2018) 1033.
14. C. Jiang, E. Hosono and H. Zhou, *Nano Today*., 1(4) (2006) 28.
15. X. Yue, W. Sun, J. Zhang, F. Wang, Y. Yang, C. Lu, Z. Wang, D. Rooney and K. Sun, *J. Power Sources.*, 331 (2016) 10.
16. P.G. Bruce, B. Scrosati and J.M. Tarascon, *Angew. Chem. Int. Ed.*, 47(16) (2008) 2930.
17. S. Yuan, Y. Zhao, W. Chen, C. Wu, X. Wang, L. Zhang and Q. Wang*, ACS Appl. Mater. Interfaces.,* 9(26) (2017) 21781.
18. G. Tian, Y. Chen, W. Zhou, K. Pan, Y. Dong, C. Tian and H. Fu, *J. Mater. Chem. A.*, 21(3) (2011) 887.
19. F. Wu, X. Wang, H. Gao, C. Hao and C. Ge, *Electrochim. Acta*., 245 (2017) 685.
20. M. Zhou, F. Pu, H. Chen, Z. Wang, H. Zhang and S. Guan, *New J. Chem*., 37(12) (2013) 4148.
21. Y. Qiu, X. Wang, H. Huang, Z. Cheng, X. Chang and L. Guo, *J. Organomet. Chem*., 880 (2019) 349.
22. Y. Ma, Z. Wang, Y. Jia, L. Wang, M. Yang, Y. Qi and Y. Bi, *Carbon*., 114 (2017) 591.

23. F. Wu, X. Wang, H. Gao, C. Hao and C. Ge, *Electrochim. Acta*., 245 (2017) 685.
*24.* J.A. Rajesh, B.K. Min, J.H. Kim, S.H. Kang, H. Kim and K.S. Ahn, *J. Electroanal. Chem*, 785 (2017) 48.
25. X. He, R. Li, J. Liu, Q. Liu, D. Song and J. Wang, *Chem. Eng. J.*, 334 (2018) 1573.
26. Y. Ma, Y. Jia, L. Wang, M. Yang, Y. Bi and Y. Qi, *J. Power Sources*, 331 (2016) 481.
27. J. Li, Q. Wu and G. Zan. *Eur. J. Inorg. Chem.*, 35 (2015) 5751.
28. Y. Qiu, H. Fan, X. Chang, H. Dang, Q. Luo and Z. Cheng, *Appl. Surf. Sci.*, 434 (2018) 16.
29. B. Senthilkumar, R.K. Selvan, L. Vasylechko and M. Minakshi, *Solid State Sci.*, 35 (2014) 18.
30. T. Yu, Z. Li, S. Chen, Y. Ding, W. Chen, X. Liu, Y. Huang and F. Kong, *ACS Sustainable Chem. Eng.*, 6(6) (2018) 7355.